Intrinsic Viscosity of Starburst Dendrimers

Chengzhen Cai and Zheng Yu Chen*

Department of Physics, University of Waterloo, Waterloo, Ontario, Canada N2L 3G1

Received May 11, 1998

Revised Manuscript Received June 29, 1998

Starburst dendrimers represent an exciting new class of macromolecular architectures as illustrated by the sketch in Figure 1.[1−5] Originally, they were synthesized by a repetitive procedure starting from a central initiator core, with each subsequent growth step creating a new "generation". Every new generation causes a doubling in monomer numbers and only a much slower increase in the overall molecular dimension. Thus, the monomer density inside a dendrimer is usually high and the growth soon saturates at a critical generation due to the packing constraint. From theoretical modeling perspective, dendrimers provide a rare opportunity for investigating a molecule densely packed within itself. The challenge is to understand the unique thermodynamic and dynamic properties of such highly dense molecules. Presently, most theoretical understandings are based on numerical modeling techniques,[6−9] and mean-field treatment.[10]

One of the extraordinary features of dendrimers lies in their intrinsic viscosity. While the intrinsic viscosities of linear and star polymers increase monotonically as molecular weight increases, the intrinsic viscosity of dendrimers displays a maximum as has been recently reported by several groups. Shown in Figure 2 by ○ and □ respectively, the maxima occur in four-generation polyether dendrimers[3] and six-generation PAMAM dendrimers.[2] Presently, the only theoretical estimation of the intrinsic viscosities was done by Mansfield and Klushin, who have claimed that they produced such maxima based on a combination of simulational and analytical approaches.[7] A recent measurement of the intrinsic viscosity of poly(propyleneimine) dendrimers, however, did not yield the maximum.[5] Other theoretical studies were based on the θ temperature Zimm[11] and Rouse approximations,[12] which are too simple to model the dynamics of dendrimer solutions. In this letter, we show that a more accurate treatment of the Mansfield−Klushin theory does not yield the anticipated maxima, and we propose a new model that provides a more reasonable explanation for the unusual behavior of the intrinsic viscosity.

The relative enhancement of the viscosity of a dilute macromolecular solution, the intrinsic viscosity $[\eta]$, is directly proportional to the friction constant ζ of monomers in solvent. Exact computation of the intrinsic viscosity of macromolecules with excluded volume and hydrodynamic interactions between monomers has been known as a formidably difficult task. Fixman developed a variational method which produces the upper and lower bounds to sandwich the "true" value of the intrinsic viscosity.[13] The formula involves (a) a "free" choice of the trial distribution function and (b) a statistical average of a combination of the inverse hydrodynamic matrix and the trial function. Interested readers may refer to the Appendix for more details.

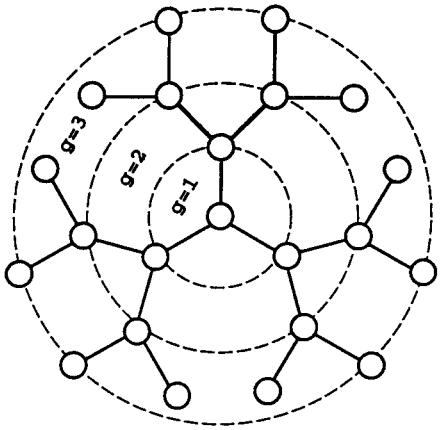

Figure 1. Sketch of a three-generation dendrimer model. The circles represent hard beads and the solid lines represent rigid rods, which can freely rotate about the branching joints. Note that this structure is defined as a two-generation dendrimer in some literatures.[3,8]

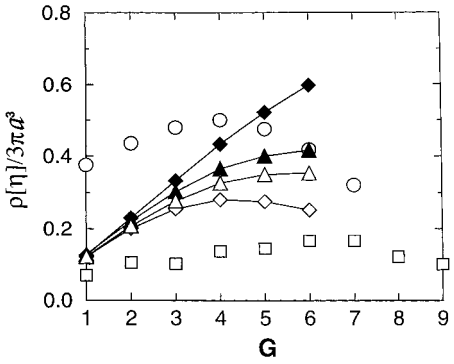

Figure 2. Reduced intrinsic viscosities $\rho[\eta]/3\pi a^3$ vs generation number G, where ρ is the weight per monomer and a is the length of the spacers. Experimental measurements for PAMAM dendrimers (a = 0.87 nm) and polyether dendrimers (a = 0.6 nm) are represented by ○ and □, respectively. Also shown are Mansfield and Klushin's calculations of upper (◆) and lower (◇) bounds, and our calculations of upper (▲) and lower (△) bounds based on the same model (see text).

Direct calculation of these bounds involves equilibrium averages of various quantities, which is a hard task by itself when the excluded volume interactions are considered. One may overcome this difficulty by resorting to the Monte Carlo simulations and numerically computing the desired quantities. Mansfield and Klushin's calculations were based on such an idea, and they further made several approximations. The first approximation in their work was to replace the hydrodynamic matrix **H** (see eq A.10), each element of which is a function of distance between two monomers, by its ensemble average $\langle \mathbf{H} \rangle$, which is a distance-independent constant matrix. This way, one does not need to invert the huge matrix for each sampled configuration, and thus the procedure saves computational time greatly. This approximation leads to the overestimate of η_U as discussed below. The second approximation was the use of kinetically generated ensembles, instead of the equilibrium ensembles, to compute the averages. The kinetic procedure was originally introduced by Lescanec and Muthukumar[6] and has been questioned recently.[9] Last, they used the center of mass as the reference center $\mathbf{r}_C$ in designing the trial functions. This ap-

S0024-9297(98)00741-4 CCC: $15.00
Published on Web 08/19/1998

proximation results in only minor numerical differences as we found. Using these approximations, they obtained the upper and lower bounds as illustrated in Figure 2 by filled and open ◇, respectively, and thus concluded that a maximum would probably occur in the intrinsic viscosity curve, according to the trend of the lower bound curve.

To test the validity of their claims, we have removed their second approximation and kept other physical conditions unchanged by using a pivot Monte Carlo algorithm, which was successfully applied to the computation of the conformational properties by one of us.[9] In numerical implementation, a dendrimer is represented by connected spherical hard beads, according to the dendritic structure in Figure 1. A trial configuration is accepted if and only if the distance between the centers of any monomer pair is greater than an excluded-volume diameter, d_e. The hydrodynamic interaction is represented by the Rotne−Prager tensor[15] in our case. The tensor is also a function of the distance between two monomers. Explicitly, a hydrodynamic parameter d_h must be introduced to describe the physics when monomers are close (see the Appendix). To repeat Mansfield and Klushin's calculation, we have used $d_e = d_h = 5a/6$, where a is the bond length. Surprisingly, our recalculations of η_L, as demonstrated by open △ in Figure 3, shift dramatically and do not display a maximum at all, up to the critical generation of about 7.

To improve the estimation of the upper bound, we decided to remove their first approximation as well and compute the thermodynamic average in eq A.10 exactly. The computation of η_U involves the inversion of a $3N \times 3N$ matrix **H**, which is computationally expensive when N is large and must be performed in each Monte Carlo step. In this work we used the Gauss−Seidel iteration method[17] with a careful choice of the initial condition rather than the more traditional LU decomposition method to invert the matrix.[16] The method is so effective that the computations can be carried out for dendrimer models up to six generations. We find that the new η_U significantly lowered the previous upper bounds and that they can now be used together with the lower bounds to bracket the "true" value of the intrinsic viscosity convincingly.

The excluded volume effects are much more severe in dendrimers than in other types of polymers. To systematically examine these effects, we have computed the variational bounds for models with $d_e = d_h = 0.25a$, $0.5a$, and $0.99a$ and generations ranging from 1 to 6 as demonstrated in Figure 3. The intrinsic viscosities predicted by a Zimm model are also included in the diagram for comparison. Our investigation indicates that neither the η_U curve nor the η_L curve goes through a maximum even for the strongest excluded volume interaction represented by $d_e = 0.99a$. Since the two curves of each set are so close to each other, it is very unlikely that the intrinsic curve, which ought to lie between them, has a maximum.

In view of the failure of the bead-rod model in explaining the maximum in the intrinsic viscosity curve, before jumping into the conclusion that more realistic potentials must be applied at the atomic level, we would like to reconsider the physical meaning of the parameters used in this simple model.

In reality, the interaction potential between two monomers typically consists of a hard-core part, which

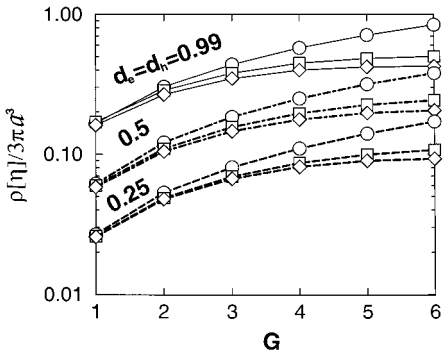

Figure 3. Estimates of intrinsic viscosities for the bead-rod model with various $d_h = d_e$: (○) Zimm model prediction; (□) η_U in eq A.10; (◇) η_L in eq A.6; solid line, $d_h = 0.99a$; dot−dashed line, $d_h = 0.5a$; long dashed line, $d_h = 0.25a$.

is represented by the hard-core diameter, and a weakly attractive part (e.g., a typical Lennard−Jones potential). Statistically, the attraction therefore compensates for a fraction of the repulsion between the monomers and the *effective* excluded volume interaction used in the Monte Carlo simulations should be represented by a diameter d_e *less* than the actual hard-core diameter. For linear chains, in the extreme case when the system is at the θ temperature, the attraction and the repulsion are completely balanced, and one practically uses $d_e = 0$ in the Monte Carlo simulations. While the Monte Carlo simulations are performed with an effective diameter d_e, there is no reason to insist that the same diameter appears in the hydrodynamic interaction tensors. As the hard-core part is more important in the hydrodynamic interactions, it is reasonable to assume that $d_e < d_h$. Figure 4 shows a set of diagrams of the variational bounds for models with various d_e's and d_h's computed by using our improved numerical technique. It can be seen from these diagrams that both η_U and η_L curves go through maxima when d_e is significantly different from d_h. In some cases, η_U at a higher generation is even smaller than η_L at a lower generation, so that we can safely say that the "true" intrinsic viscosity curve also has a maximum at a certain generation.

It should be noted that the cases where $d_e = 0$ actually represent the θ condition, which were considered by La Ferla in a recent work with the Zimm approximation.[11] It is not difficult to show that the intrinsic viscosity predicted by the Zimm model is expressed in eq A.11, coincident with the pre-averaged approximation of η_U. As shown in Figure 4 by ○, the Zimm model provides rather poor estimates for the intrinsic viscosity of starburst dendrimers. Whether or not a θ temperature actually exists in dendrimers in reality is questionable,[18] and beyond the scope of the current study.

The experimental data shown in Figure 2 were converted to our scale. The $[\eta]$ curves of PAMAM and polyether dendrimers behave similarly to some of our curves in Figure 4. We do not intend to *quantitatively* compare these experimental results with our estimates due to the complications that may arise in real dendrimers. These include the flexibility of chemical bonds (the "spacers" are less rigid in PAMAM dendrimers than that in polyether dendrimers), the difference between the sizes of monomers (the branching center could be larger than other units in polyether dendrimers),[3] and the determination of the actual d_h and d_e (one might even argue that different d_e and d_h should be used for

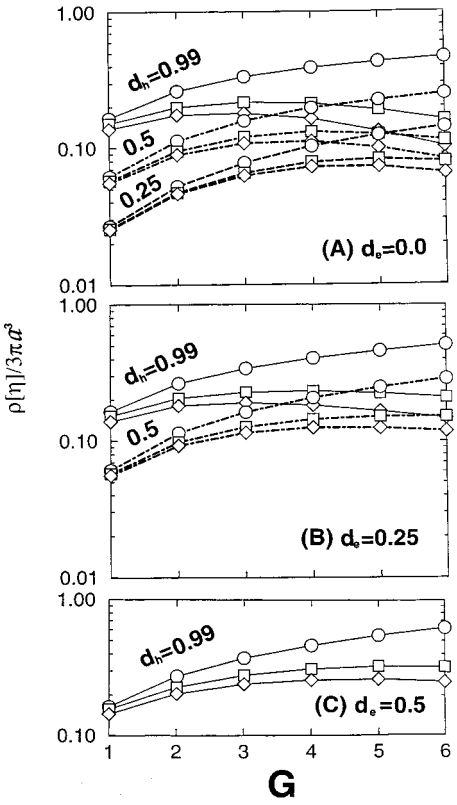

Figure 4. Estimates of intrinsic viscosity for the bead-rod model with $d_h > d_e$: (○) the Zimm model prediction; (□) η_U in eq A.10; (◇) η_L in eq A.6; solid line, $d_h = 0.99a$; dot−dashed line, $d_h = 0.5a$; long dashed line, $d_h = 0.25a$.

different generations). The qualitative agreement between the experimental results and our estimates is already quite encouraging. It also becomes clear why the intrinsic viscosity curve of some dendrimers [e.g. poly(propylene imine)] does not display a maximum, as indicated by some of our curves.

In this work, we estimated the intrinsic viscosity of dendrimer models by Fixman's variational treatment. In contrast to previous claims, we found that more accurate estimates of the intrinsic viscosity of a customarily used bead-rod model failed to explain experimental observations. We also found that the Zimm model gave rather poor approximations for the intrinsic viscosities of dendrimers. Finally, we proposed a new model in which the excluded volume interaction used for the equilibrium averages is represented by a diameter smaller than the hard-core diameter used in hydrodynamic interaction tensors. This model can be used to explain the unique behavior of the intrinsic viscosity of starburst dendrimers.

A. Appendix. Consider a macromolecular solvent under a shear flow represented by the velocity vector, $\mathbf{V}(\mathbf{r}) = \kappa \hat{\mathbf{e}}_\alpha \hat{\mathbf{e}}_\beta \cdot \mathbf{r}$, where $\hat{\mathbf{e}}_\alpha, \hat{\mathbf{e}}_\beta$ are any two of the three bases of the Cartesian coordinates.

According to Fixman, the lower bound η_L is expressed as a functional of a trial function Φ:[13,14]

$$\eta_L = -\frac{{k_B}^2 T^2}{\zeta \eta_s \kappa^2 N} \sum_{j,k} \langle \nabla_j \Phi \cdot \mathbf{H}_{jk} \cdot \nabla_k \Phi \rangle + \frac{2k_B T}{\eta_s \kappa^2 N} \sum_j \langle \nabla_j \Phi \cdot \mathbf{V}_j \rangle \tag{A.1}$$

where N is the total number of monomers, η_s is the solvent viscosity, ζ is the effective friction constant, $\boldsymbol{V}_j = \boldsymbol{V}(\mathbf{r}_j)$ is the velocity field felt by the jth monomer at $\mathbf{r}_j$, $\langle \cdot \rangle$ denotes the equilibrium average and $\Phi(\mathbf{r}_1, ..., \mathbf{r}_N)$ satisfies

$$\sum_j \nabla_j \Phi = 0 \tag{A.2}$$

The solvent-mediated hydrodynamic interactions between monomers j and k can be effectively modeled by the Rotne-Prager tensor[15]

$$\mathbf{H}_{jk} = \delta_{jk}\mathbf{I} + \frac{1 - \delta_{jk}}{16 d_h {r_{jk}}^3} \begin{cases} {d_h}^2((6r_{jk} + {d_h}^2)\mathbf{I} + (6r_{jk}^2 - 3{d_h}^2)\hat{\mathbf{r}}_{jk}\hat{\mathbf{r}}_{jk}) & (r_{jk} > d_h) \\ {r_{jk}}^3(16d_h - 9r_{jk})\mathbf{I} + 3{r_{jk}}^4 \hat{\mathbf{r}}_{jk}\hat{\mathbf{r}}_{jk} & (r_{jk} < d_h) \end{cases} \tag{A.3}$$

where r_{jk} is the magnitude and $\hat{\mathbf{r}}_{jk}$ is the unit vector of $\mathbf{r}_j - \mathbf{r}_k$ and d_h is the hard-core diameter of each monomer. At a steady state, the perturbed system reaches a distribution function different from the equilibrium counterpart. η_L becomes $[\eta]$ itself when Φ is exact. Fixman, and Doi and Edwards have suggested the use of a polynomial of second rank in $\mathbf{r}$ for Φ. In this work, we adopt a similar trial function

$$\Phi = 1 + \xi \sum_{j,k} (r_{j\alpha} - r_{C\alpha})(H^{-1})_{jk}(r_{k\beta} - r_{C\beta}) \tag{A.4}$$

where ξ is a constant to be determined by optimizing the corresponding lower bound, and H is the preaveraged version of $\mathbf{H}$ such that $H_{jk} = \mathrm{Tr}\langle \mathbf{H}_{jk} \rangle/3$, where the trace is taken in the 3-dimensional Cartesian space. Many authors have used the center of mass as the reference center $\boldsymbol{r}_C$, but we found that it is more reasonable to use

$$\mathbf{r}_C = \frac{\sum_{j,k}(H^{-1})_{jk}\mathbf{r}_k}{\sum_{j,k}(H^{-1})_{jk}} \tag{A.5}$$

since the Zimm model resembles a collection of beads with mass matrix H^{-1} and the effective center of mass is thus given by eq A.5.[16] Substituting eq A.4 into the right-hand side of eq A.1 and then maximizing η_L with respect to ξ, we have

$$\eta_L = \frac{\xi}{\eta_s N} \frac{(\sum_{j,k}\langle \mathbf{u}_j \cdot (H^{-1})_{jk}\mathbf{u}_k \rangle)^2}{\sum_{j,k,m,n}\langle \mathbf{u}_j (H^{-1})_{jk} \cdot \mathbf{H}_{km} \cdot (H^{-1})_{mn}\, \mathbf{u}_n \rangle} \tag{A.6}$$

where $\mathbf{u}_j = {}^1/_2(\hat{\mathbf{e}}_\alpha \hat{\mathbf{e}}_\beta + \hat{\mathbf{e}}_\beta \hat{\mathbf{e}}_\alpha) \cdot (\mathbf{r}_j - \mathbf{r}_C)$.

The general formula for the variational upper bound is[13,14]

$$\eta_U = \frac{1}{\eta_s \kappa^2 N} \sum_{j,k} \langle (\mathbf{V}_j^* - \mathbf{V}_j) \cdot (\mathbf{H}^{-1})_{jk} \cdot (\mathbf{V}_k^* - \mathbf{V}_k) \rangle \tag{A.7}$$

where $\mathbf{H}^{-1}$ is the inverse of $\mathbf{H}$ such that $\sum_l (\mathbf{H}^{-1})_{jl} \cdot \mathbf{H}_{lk} = \delta_{jk}\mathbf{I}$, and $\mathbf{V}_j^*$'s are another set of trial functions satisfying

$$\sum_j \nabla_j \cdot (\Psi_{eq} \mathbf{V}_j^*) = 0 \tag{A.8}$$

with Ψ_{eq} the equilibrium distribution function. Accord-

ing to Fixman's proposal, we adopt a linear form in $\boldsymbol{r}$

$$\mathbf{V}_j^* = -\kappa \hat{\mathbf{e}}_\alpha \hat{\mathbf{e}}_\beta \cdot \mathbf{r}_C + \frac{\kappa}{2} \hat{\mathbf{e}}_\gamma \times (\mathbf{r}_j - \mathbf{r}_C) \qquad \text{(A.9)}$$

where, again, $\boldsymbol{r}_C$ is given by eq A.5 rather than the center of mass. One may verify that eq A.9 satisfies eq A.8 by direct substitution. Hence

$$\eta_U = \frac{\zeta}{\eta_s N} \sum_{j,k} \langle \mathbf{u}_j \cdot (\mathbf{H}^{-1})_{jk} \cdot \mathbf{u}_k \rangle \qquad \text{(A.10)}$$

The Zimm model is equivalent to a system with a constant hydrodynamic interaction matrix. Replacing **H** by its ensemble average in both eq A.6 and eq A.10, we find that $\eta_L = \eta_U = \eta_Z$ where

$$\eta_Z = \frac{\zeta}{\eta_s N} \sum_{j,k} \langle \mathbf{u}_j \cdot (H^{-1})_{jk} \mathbf{u}_k \rangle \qquad \text{(A.11)}$$

References and Notes

(1) Tomalia, D. A.; Baker, H.; Dewald, J.; Hall, M.; Kallos, G.; Martin, S.; Roeck, J.; Ryder, J.; Smith, P. *Polym. J. (Tokyo)* **1985**, *17*, 117. Tomalia, D. A.; Baker, H.; Dewald, J.; Hall, M.; Kallos, G.; Martin, S.; Roeck, J.; Ryder, J.; Smith, P. *Macromolecules* **1986**, *19*, 2466. Tomalia, D. A.; Naylor, A. M.; Goddard, W. A., III, *Angew. Chem., Int. Ed. Engl.* **1990**, *29*, 138. Hawker, C. J.; Fréchet, J. M. J. *J. Chem. Soc., Chem. Commun.* **1990**, 1010. Hawker, C. J.; Fréchet, J. M. J. *J. Am. Chem. Soc.* **1990**, *112*, 7638. Hawker, C. J.; Fréchet, J. M. J. *Macromolecules* **1990**, *23*, 4726. Newkome, G. R.; Lin, X. *Macromolecules* **1991**, *24*, 1443. Morikawa, A.; Kakimoto, M.; Imai, Y. *Macromolecules* **1991**, *24*, 3469. Moreno-Bondi, M. C.; Orellana, G.; Turro, N. J.; Tomalia, D. A. *Macromolecules* **1990**, *23*, 910.

(2) Tomalia, D. A.; Hedstrand, D. M.; Wilson, L. R. *Encyclopedia of Polymer Science and Engineering*, 2nd ed.; Wiley: New York, 1990.

(3) Mourey, T. H.; Turner, S. R.; Rubinstein, M.; Fréchet, J. M. J.; Hawker, C. J.; Wooley, K. L. *Macromolecules* **1992**, *25*, 2401.

(4) Fréchet, J. M. J. *Science* **1994**, *263*, 1710.

(5) Scherrenberg, R.; Coussens, B.; van Vliet, P.; Edouard, G.; Brackman, J.; de Brabander, E.; Mortensen, K. *Macromolecules* **1998**, *31*, 456.

(6) Lescanec, R. L.; Muthukumar, M. *Macromolecules* **1990**, *23*, 2280.

(7) Mansfield, M. L.; Klushin, L. I.; *J. Phys. Chem.* **1992**, *96*, 3994. This reference also contains calculations for models with extra monomers between the branching units. In our case, a similar computation would cost unrealistic CPU times even by our new algorithm. These models are thus not considered here.

(8) Murat, M.; Grest, G. S. *Macromolecules* **1996**, *29*, 1278.

(9) Chen, Z. Y.; Cui, S. *Macromolecules* **1996**, *29*, 7943.

(10) de Gennes, P. G.; Hervet, H. *J. Phys. (Paris)* **1983**, *44*, L351. Boris, D.; Rubinstein, M. *Macromolecules* **1996**, *29*, 7251.

(11) La Ferla, R.; *J. Chem. Phys.* **1997**, *106*, 688.

(12) Cai, C.; Chen, Z. Y. *Macromolecules* **1997**, *30*, 5104.

(13) Fixman, M. *J. Chem. Phys.* **1983**, *78*, 1588.

(14) Doi, M.; Edwards, S. F. *The theory of polymer dynamics*; Clarendon, Oxford, England 1986.

(15) Rotne, J.; Prager, S. *J. Chem. Phys.* **1969**, *50*, 4831.

(16) Cai, C.; Chen, Z. Y. Unpublished material.

(17) Sewell, G. *Computational methods of linear algebra*; Ellis Horwood: New York, 1990.

(18) Douglas, J. F.; Roovers, J.; Freed, K. F. *Macromolecules* **1990**, *23*, 4618. Ganazzoli, F. *Macromolecules* **1992**, *25*, 7357.

MA9807419